NIH Public Access
Author Manuscript
Mol Microbiol. Author manuscript; available in PMC 2014 October 01.

Published in final edited form as:
Mol Microbiol. 2013 October ; 90(2): 338–355. doi:10.1111/mmi.12367.

A nucleolar AAA-NTPase is required for parasite division

Elena S. Suvorova[1], **Joshua B. Radke**[1], **Li-Min Ting**[4,5], **Sumiti Vinayak**[2], **Carmelo A. Alvarez**[1], **Stella Kratzer**[1], **Kami Kim**[4,5], **Boris Striepen**[2,3], and **Michael W. White**[1]

[1]Departments of Molecular Medicine & Global Health, University of South Florida, Tampa, FL 33612

[2]Center for Tropical and Emerging Global Diseases, University of Georgia, Athens, GA 30602

[3]Department of Cellular Biology, University of Georgia, Athens, GA 30602

[4]Department of Medicine, Albert Einstein College of Medicine, Bronx, NY 10461

[5]Department of Microbiology & Immunology, Albert Einstein College of Medicine, Bronx, NY 10461

Summary

Apicomplexa division involves several distinct phases shared with other eukaryote cell cycles including a gap period (G1) prior to chromosome synthesis, although how progression through the parasite cell cycle is controlled is not understood. Here we describe a cell cycle mutant that reversibly arrests in the G1 phase. The defect in this mutant was mapped by genetic complementation to a gene encoding a novel AAAATPase/CDC48 family member called TgNoAP1. TgNoAP1 is tightly regulated and expressed in the nucleolus during the G1/S phases. A tyrosine to a cysteine change upstream of the second AAA+ domain in the temperature sensitive TgNoAP1 allele leads to conditional protein instability, which is responsible for rapid cell cycle arrest and a primary defect in 28S rRNA processing as confirmed by knock-in of the mutation back into the parent genome. The interaction of TgNoAP1 with factors of the snoRNP and R2TP complexes indicates this protein has a role in pre-rRNA processing. This is a novel role for a cdc48-related chaperone protein and indicates that TgNoAP1 may be part of a dynamic mechanism that senses the health of the parasite protein machinery at the initial steps of ribosome biogenesis and conveys that information to the parasite cell cycle checkpoint controls.

Keywords

Apicomplexa; *Toxoplasma gondii*; cell cycle; nucleolus; G1 phase; replication; AAA-ATPase

Introduction

Toxoplasma gondii infections are a health risk for millions of individuals that contact this pathogen annually, particularly those with immune systems weakened by aging, chemotherapy or AIDS; and women that acquire their first infection during pregnancy. Uncontrolled parasite growth that occurs in these patients can lead to significant tissue destruction and associated inflammation resulting in the disease toxoplasmosis. The basic link between parasite growth and pathogenesis in toxoplasmosis is a shared principle of

[*]**Address correspondence to:** Michael W. White Florida Center of Drug Discovery and Innovation Department of Global Health University of South Florida 3720 Spectrum Blvd, Suite 304 Tampa, FL 33612 mwhite.usf@gmail.com office 813-974-8411 Fax 813-974-0804.

NIH-PA Author Manuscript
NIH-PA Author Manuscript
NIH-PA Author Manuscript

NIH-PA Author Manuscript

NIH-PA Author Manuscript

NIH-PA Author Manuscript

other apicomplexan-caused diseases, with the corollary that the most effective treatments are able to reduce parasite burden in afflicted individuals.

Highly efficient asexual replication is critical to the ability of Apicomplexans to spread infection throughout their hosts. A series of recent studies have now defined the basic biogenic steps of parasite replication that are in common with mitotic cell cycles of eukaryotic model organisms like yeast (Gubbels *et al.*, 2008b, Striepen *et al.*, 2007). Definable transitions from G1 to S phase and S to mitosis are observed that are in principle similar to other eukaryotic cell cycles. By contrast, mitosis and cytokinesis is very unusual in these parasites both with respect to the extensive nuclear reduplication that occurs in some species as well as the peculiar biosynthetic events required for building the parasite invasion apparatus that concludes every round of division. There is evidence these general and specialized processes are coordinated (Gubbels *et al*., 2008b), although the molecular mechanisms responsible are largely unknown. Apicomplexan parasites progress through cell division on a well ordered path in which chromosomal DNA synthesis follows a lengthy gap phase. The Gap 1 phase (G1) in the Apicomplexa has defined boundaries and as in other eukaryotes, this period is devoted to renewing the machinery required for DNA and protein synthesis (Behnke *et al.*, 2010, Bozdech *et al.*, 2003). Here again the mechanisms regulating the parasite G1 period are not understood as many of the key checkpoint factors that control G1 to S phase progression in yeast or higher eukaryotes are absent from the Apicomplexa (Behnke *et al*., 2010, Gubbels *et al*., 2008b). The G1 phase in the Apicomplexa is important to disease as it provides a means for these parasites to avoid the host immune response and for achieving viable long-term dormancy in the environment. This latter feature is best characterized for the G1-like state of the sporozoite (Radke *et al*., 2001), which for some family members of the *Eimeria spp*. may lead to survival outside the host for months to years. Coccidian sporozoites residing in the mature oocyst are cells with a single nucleus and haploid chromosome content (Radke *et al*., 2001). In other Apicomplexa, the ability to pause in a G1/G0 state allows long-term residence in the intermediate host, such as the liver hypnozoite of *Plasmodium vivax* or the tissue cyst (bradyzoite) of *Toxoplasma gondii*. These are not terminal states and upon stimulation the parasite easily resumes replication causing disease recrudescence. A temporary G1 or G0 state in these parasites also may contribute to drug resistance (Teuscher *et al.*, 2012, Tucker *et al.*, 2012). The appearance of artemisinin resistant strains of *Plasmodium falciparum* in Southeast Asia is associated with the induction of a ring-like form, which may be equivalent to the early G1 stage of the intraerythrocytic division cycle. The removal of drug pressure allows these parasites to quickly recommence replication leading to recrudescence of disease in these patients (Teuscher *et al*., 2012, Tucker *et al*., 2012). There are few drugs in use that are effective against G1/G0 stages of Apicomplexa life cycles, which is in part reflected in the lack of knowledge of how these cell cycle transitions are regulated.

To address fundamental mechanisms of cell cycle control in apicomplexan parasites, we have isolated a large collection of temperature sensitive mutants in *Toxoplasma* and have begun to identify the defective genes in specific mutants using new forward genetic approaches (Gubbels *et al.*, 2008a). The diversity of mutants in this collection that conditionally arrest at specific positions throughout the parasite cell cycle supports the hypothesis that checkpoints control multiple transitions in the apicomplexan division cycle. In this study, we characterize a mutant (11-104A4) from this collection that at high temperature arrests in the parasite G1 phase. The protein defective in this mutant is a cell cycle regulated AAA-ATPase that resides exclusively in the parasite nucleolus. This novel AAA-ATPase in *Toxoplasma* is essential for cell cycle progression, and is one of the first factors established in this parasite that is associated with checkpoint regulation of G1 to S phase progression.

NIH-PA Author Manuscript

NIH-PA Author Manuscript

NIH-PA Author Manuscript

Results

A temperature-sensitive mutant growth arrests in the G1 phase

Tachyzoite clone 11-104A4 was isolated from a chemical mutagenesis screen for cell cycle mutants in *Toxoplasma* (Gubbels *et al*., 2008a). Mutant 11-104A4 parasites followed a pattern of temperature sensitive growth with replication at 34°C and growth arrest at 40°C (Fig. S1A). A shift to the restrictive temperature rapidly arrested growth in the first or second cell cycle post-invasion (54% ones, 45% twos, 0% fours at 10 h) and was fully reversible during this short timeframe (≤ 8 h, Fig. S1B), while longer incubations at 40°C led to a progressive loss of parasite viability (approximately 45% ones, 35% twos, 20% fours per vacuole at 24 - 72 h). Immunofluorescence analysis (IFA) of mutant 11-104A4 parasites using markers for the centrosome (Centrin1), the centrocone (MORN1), daughter scaffolds (IMC1), and nuclear DNA placed the growth arrest in the G1 phase of the cell cycle (Fig. 1A, 90% G1 parasites at 24 h, 40°C). Parasites arrested at 40°C possessed one nucleus and a single centrosome consistent with the G1 subcellular organization (Radke *et al*., 2001), and this cell cycle assignment was supported by the single nuclear spindle pole per nucleus (Fig. 1A, MORN1 staining) (Gubbels *et al.*, 2006). Interestingly, the defect in this mutant also led to an increase in parasite cell size and a change in shape from elongated to more rounded (Fig. 1A and B, IMC1 staining; also Fig. S1C-quantification), which was distinct from previously studied G1 mutants in *Toxoplasma* (Gubbels *et al*., 2008a) (Suvorova and White, unpublished). We noted a 35% increase in the parasite cell diameter that appeared to be mostly due to enlargement of the nucleus and nucleolus. The increase in nucleolar volume in mutant 11-104A4 grown at 40°C was visualized by staining parasites with antibodies against nucleolar transcription factor TgNF3 (Fig. 1B and C), which occupies both the fibrillar core and part of the outer granular ring of the nucleolus (Olguin-Lamas *et al.*, 2011). The single apicoplast in mutant parasites at 40°C was shifted to a more anterior location as was the rhoptry organelles likely as a consequence of the increased nuclear size (Fig. 1A). To validate the G1 phase arrest, we evaluated gene expression of mutant 11-104A4 parasites at the permissive and restricted temperatures by microarray analysis, and compared these data to the unique G1 and S/M subtranscriptomes that characterize the tachyzoite cell cycle transcriptome (Behnke *et al*., 2010). As expected for a G1 phase arrest, the mRNA pools at high temperature in the mutant parasites (Fig. 2A) showed higher levels of transcripts that normally peak in G1 (red dots) than S/M peak transcripts (blue dots) when compared to mutant parasites grown at the permissive temperature (see full gene lists in Dataset S1). The transcriptome of mutant 11-104A4 parasites grown at the permissive temperature was comparable to the parent strain grown at 34°C (Fig. 2B) and was consistent with the mRNA profiles expected for asynchronously growing populations.

Genetic complementation identifies a defective nucleolar ATPase that is responsible for the failure of mutant 11-104A4 to progress through the G1 phase

To discover the genetic lesion in mutant 11-104A4, we genetically complemented the mutant with DNA from a RH strain cosmid genomic library (Gubbels *et al*., 2008a). Mutant parasites were transfected with library cosmids and selected with pyrimethamine at 40°C. Genomic DNA from double positive populations (temperature and drug resistant) was isolated and fragments of the integrated cosmid inserts recovered using marker rescue techniques (Gubbels *et al*., 2008a, Suvorova *et al.*, 2012). Sequencing of the recovered DNA fragments identified a region on chromosome VIII between 961,798bp and 1,000,661bp that contains four predicted genes (Fig. 3A). The complementing locus was resolved further by transformation of mutant 11-104A4 with DNA from adjacent tiled cosmid clones (TOXOV53 and PSBLD53). This second complementation of the 11-104A4 mutant with individual cosmids demonstrated that gene 3 or 4, but not gene 1 or 2 was sufficient to

NIH-PA Author Manuscript

NIH-PA Author Manuscript

NIH-PA Author Manuscript

rescue mutant growth at high temperature. DNA fragments encompassing gene TGGT1_117040 (gene 4) amplified by PCR from parental genomic DNA, but not from mutant DNA were able to fully rescue the temperature defect of mutant 11-104A4 (Fig. 3A). Gene TGGT1_117040 encodes a 1,326 amino acid protein containing two conserved P-loop NTPase domains (see diagram Fig. S2A). Sequencing of TGGT1_117040 cDNA from mutant 11-104A4 and the parental RHΔ*hxgprt* strain revealed a point mutation (TAC to TGC) changing a tyrosine residue into a cysteine (Y984C, Fig. 3A) immediately upstream of the second AAA+ domain (Fig. S2A). The protein encoded by gene TGGT1_117040 belongs to the AAA+ family of proteins involved in a wide range of processes, including DNA replication, ribosome biogenesis, protein degradation, membrane fusion, microtubule severing, peroxisome biogenesis, signal transduction and the regulation of gene expression (White & Lauring, 2007). Phylogenetic analysis with similar proteins from other eukaryotes indicated that *Toxoplasma* gene TGGT1_117040 encodes a factor related to nucleolar AAA +-proteins, human NVL2 and yeast Rix7 (Fig. 3B, green box, see also alignment Fig. S3). This group of AAA ATPases is related to a family of canonical cell cycle regulators, cdc48/ VCP proteins (Fig. 3B, blue box). However, the absence of the unique N-terminal cdc48-domain in the yeast Rix7/human NVL2 group (Niwa *et al.*, 2012) distinguishes these nucleolar AAA-ATPase proteins from the canonical cdc48/VCP family (not shown).

Consistent with the phylogenetic assignment of this factor, we found that native TGGT1_117040 protein was localized to the tachyzoite nucleolus. Clone $C6^{wt}$ expresses an epitope tagged copy of this protein produced by genetic knock-in (Huynh & Carruthers, 2009) of a triple repeated myc tag fused to the C-terminal end of the last exon in the TGGT1-117040 gene locus of the RHΔ*ku80* parental strain (Fig. 3C). Nucleolar localization was established using co-staining with nucleolar markers fibrillarin (Fig. 3C) and TgNF3 (Fig. S2B). Like the majority of eukaryotes, apicomplexan parasites are predicted to have a bipartite nucleolus consisting of a fibrillar core and a granular outer compartment (Thiry & Lafontaine, 2005). Antibody against the core protein fibrillarin confirmed the presence of this distinctive central region in the *Toxoplasma* nucleolar structure (Fig. 3C, red stain). The TGGT1_117040 tagged protein appeared to wrap the fibrillarin core (inset Fig. 3C) suggesting this protein was primarily in the granular ring of the nucleolus. Based on the localization of this factor within the parasite nucleolus, we have named this protein *Toxoplasma gondii* nucleolus-associated protein 1 (TgNoAP1).

To verify that the Y984C change in mutant ts-TgNoAP1 was responsible for temperature sensitive growth of mutant strain 11-104A4, we genetically introduced the Y984C mutation into RHΔ*ku80* parasites through exon replacement, while also fusing a triple myc epitope to the C-terminal end of the Y984C converted protein (Huynh & Carruthers, 2009). A similar introduction of the 3xmyc epitope tag into the native TgNoAP1 gene locus ($TgNoAP1^{myc}$ protein) in transgenic clone $C6^{wt}$ did not lead to high temperature sensitivity ($C6^{wt}$, Fig. 3D, blue curves). By contrast, the growth of clones where the Y984C mutation was introduced became conditional for temperature similar to the original 11-104A4 mutant (see clone $F10^{Y984C}$, Fig. 3D and S1A, red curves). The mutant ts-$TgNoAP1^{myc}$ protein was readily detected in the nucleolus of $F10^{Y984C}$ parasites grown at 34°C, while upon shift to 40°C this factor rapidly disappeared (Fig. 3E). Western blot analysis of the total lysates of $C6^{wt}$ and $F10^{Y984C}$ parasites grown at 34°C and 40°C verified substantial reduction of ts-$TgNoAP1^{myc}$ protein levels at the restricted temperature (Fig. 3F). Thus, instability of the mutant ts-$TgNoAP1^{myc}$ protein likely is the major contributor to the severe growth defects in the $F10^{Y984C}$ clone. These results also demonstrate that when cultured at higher temperatures clone $F10^{Y984C}$ and the original mutant 11-104A4 parasites are *de facto* null mutants due to the loss of ts-TgNoAP1 protein. Altogether, these data provided strong evidence that the Y984C mutation identified in the ts-TgNoAP1 gene sequence of the original 11-104A4 strain was responsible for conditional growth arrest in the G1 phase.

NIH-PA Author Manuscript

NIH-PA Author Manuscript

NIH-PA Author Manuscript

TgNoAP1 protein has two conserved AAA-domains comprised of the Walker A P-loop and Walker B signature motifs (Fig. S2A). The conservative lysine residue in the Walker A motif is known to reside in the ATP binding pocket and is essential for ATPase enzymatic activity of these proteins (Briggs *et al.*, 2008, Rouiller *et al*., 2002). To investigate whether ATPase activity is required for TgNoAP1 function, we constructed ATPase dead mutant by replacing two conservative lysines in the both Walker A domains, K495 and K992, with alanines (Fig. S2A). We then tested ability of this dead ATPase mutant to rescue temperature-sensitive growth of the mutant 11-104A4. Unlike wild type allele, the K495A/K992A mutant failed to rescue ts-TgNoAP1 parasites at 40°C, indicating that the ATPase activity of the factor is required for cell cycle function in *Toxoplasma*.

Major morphogenic changes to the nucleolus accompany tachyzoite cell division

The nucleolus localization of TgNoAP1, lead us to explore the cell cycle changes associated with this nuclear compartment in parent and mutant parasites. To provide a morphological context to understand the dynamics of TgNoAP1 nuclear expression, we co-stained tachyzoites for nucleolar factor TgNF3 and also IMC1, which was included to identify the cell cycle position of individual parasites (Fig. 4). The single nucleolus of G1 and S phase tachyzoites stained by TgNF3 had a central location within the parasite nucleus and was not stained by DAPI (Fig. 4 top two image panels). In late S phase (Fig. 4, early buds) dynamic nucleolar fragmentation first was evident coincident with the onset of mitosis and daughter budding (Olguin-Lamas *et al*., 2011). Assembly and expansion of new nucleoli paralleled daughter bud development (Fig. 4, bottom three panels), accompanied by the occasional loss of nucleolar material in the residual mass (see starred bodies in bottom panels). The discard of excess cellular material is a mechanism thought to be involved in regulating parasite size (Conde de Felipe *et al*., 2008). In multicellular eukaryotes undergoing open mitosis, fragmentation of nucleolus reflects a normal remodeling of the nucleolus (Hernandez-Verdun, 2011). Nucleolar fragments are assimilated into the process of disassembly of the nuclear structure, and while apicomplexan protozoa division is endomitotic, they appear to have preserved this mechanism to ensure that a nucleolar organelle is available for each daughter parasite.

Placed within the context of nucleolar morphogenesis, TgNoAP1^{myc} fusion protein tagged in the endogenous locus of the parental RH strain was tightly cell cycle regulated with maximum levels of expression in G1 and early S phase parasites (Fig. 5A, see also G1/mitosis comparison in Fig. S2C). The distinctive ring pattern of TgNoAP1^{myc} indicative of localization in the granular ring was also present in G1 and S phase parasites (Fig. 5A, inset merged images). In late S phase, TgNoAP1^{myc} was rapidly downregulated (Fig. 5A) coincident with the major morphogenic fragmentation and reassembly of the nucleolus organelle (Fig. 4). During this specific cell cycle transition, TgNoAP1^{myc} disengaged from the nucleolus and gradually lost connection to the nucleolar core that retains fibrillarin protein (Fig. 5B). The TgNoAP1^{myc} association with the granular ring was re-established in the newly formed nucleolar organelle of the next G1 phase (Fig. 5A, inset image, G1 panel) as expression of this factor once again reaches maximum levels. The cell cycle expression of TgNoAP1^{myc} has the same cyclical profile as the native TgNoAP1 mRNA profile, which was also maximally expressed in G1 (Fig. S2D). Importantly, the timing of maximum TgNoAP1 expression in G1 correlates well with the cell cycle phenotype of mutant 11-104A4 parasites growth arrested at the restricted temperature.

In mutant populations lacking ts-TgNoAP1 at the high temperature, we observed only a single nuclear morphology that was consistent with an enlarged G1 organelle (Fig. 1). The increase in nucleolar volume in mutant parasites did not appear to disrupt key compartmental boundaries with fibrillarin still localized to the central core region (Fig. 5C)

NIH-PA Author Manuscript

NIH-PA Author Manuscript

NIH-PA Author Manuscript

and other nucleolar residential protein TgNF3 also properly localized in these growth arrested parasites (Fig. 1B). The expansion of the granular compartment appeared to be largely responsible for this increase as the fibrillarin core was unchanged by temperature (Fig. 5C and D), while the organelle volume stained by αTgNF3 antibodies increased (Fig. 1C). Altogether, these observations suggest that the nature of TgNoAP1 function in the nucleolus is different from other residential proteins and TgNoAP1 is likely not involved in the maintenance of structural integrity or replication of the nucleolus. The distinct cell cycle changes of TgNoAP1^{myc} when compared to the constitutive profiles of other nucleolar proteins such as fibrillarin demonstrates that some but not all nucleolar factors are subject to dynamic regulatory mechanisms that appear linked to major cell cycle transitions.

Neither catastrophic loss of ribosome content nor a block to chromatin-end maintenance explains the rapid cell cycle arrest of ts-TgNoAP1 mutant parasites

Among the known functions for nucleolar AAA+-proteins is aiding 60S ribosome subunit assembly and transport (Kressler *et al.*, 2012, Kressler *et al.*, 2008, Nagahama *et al.*, 2004, Nagahama *et al.*, 2006). Yeast ortholog Rix7 is an essential nucleolar protein that is required for maturation of the pre-60S particle (Gadal *et al.*, 2001, Kressler *et al.*, 2008), therefore, we examined whether ribosome components were affected by the loss of ts-TgNoAP1. We first explored the total RNA content of mutant 11-104A4 parasites grown for 24 h at two temperatures (34°C versus 40°C) using a microfluidic NanoChip. The major subunit rRNA species (28S and 18S) were present in all these parasites, however, a reproducible decrease in the 28S/18S rRNA ratio was observed in RNA preparations from mutant parasites grown at 40°C as compared to parental controls (Fig. 6A). This ratio was restored to normal levels in a clone genetically rescued with cosmid TOXOV53 (40^{C} ratio compared to mutant parasites at 34°C are similar, Fig. 6A). These data indicated that rRNA transcription and/or processing was conditionally affected by temperature in mutant 11-104A4 parasites. To determine whether the apparent decrease in 28S rRNA translated into a major loss of ribosomes, we evaluated the expression of the large subunit protein TgRPL36 (TGGT1_052600) in the mutant parasites. TgRPL36 was chosen for C-terminal tagging with triple myc epitope, as this ribosomal protein will tolerate modification without loss of ribosome function (Sanz *et al.*, 2009). In contrast to the change in rRNA levels, ectopically expressed in either parental RHΔ*hxgprt* or mutant 11-104A4 parasites, the TgRPL36^{myc} fusion protein was present in the cytoplasm of both strains at levels unaffected by temperature (24 h post-temperature shift, Fig. 6B and C). To ensure that TgRPL36^{myc} protein was assembled into ribosomes at the non-permissive temperature, we evaluated ribosome profiles of mutant and parental parasites by sucrose gradient sedimentation. Cytoplasmic lysates were prepared from mutant 11-104A4 and RHΔ*hxgprt* parasites cultured at 40°C for 10 h, which was the timeframe required to fully arrest 11-104A4 parasites in G1, while the parent strain had initiated log phase growth (Fig. S1A). Lysates were applied to 15-40% sucrose gradients and centrifuged using a timeframe that readily resolves RNP particles and ribosomal subunits from translationally active polysomes (see Experimental Procedures) (White *et al.*, 1987). The analysis of total RNA and TgRPL36^{myc} expression in these gradients showed a very similar distribution of ribosome subunits and polysomes in mutant and parental samples (Fig. 6D). Importantly, these results provided solid evidence that TgRPL36^{myc} was expressed, assembled into ribosome subunits, and these TgRPL36-containing subunits were loaded onto mRNA in mutant parasites at high temperature. Thus, the loss of the ts-TgNoAP1 factor at 40°C in mutant 11-104A4 parasites that leads to rapid growth arrest did not appear to be caused by a rapid catastrophic loss of ribosomes or polyribosomes.

In yeast, Rix7 is known to regulate cycling of pre-60S associated factor Nsa1 between nucleoplasm and cytoplasm, which was essential step in maturation of the large subunit of

NIH-PA Author Manuscript

NIH-PA Author Manuscript

NIH-PA Author Manuscript

ribosome (Kressler *et al*., 2008). We identified and ectopically expressed the *Toxoplasma* ortholog of Nsa1/Wdr74 (TgWdr74: TGGT1_080560, see Fig.S4A for protein alignment). As expected TgWdr74^{myc} was exclusively localized to the tachyzoite nucleolus (Fig. S4B). However, in contrast to yeast *rix7* mutants, localization of TgWdr74^{myc} in *Toxoplasma* was unaffected by the disappearance of ts-TgNoAP1 at high temperature (Fig. S4B). Furthermore, we did not observe the 35S precursor rRNA molecules in the mutant total RNA preparations (Fig. 6A and D) that are known to accompany the block to 60S biosynthesis in *rix7* mutants (Gadal *et al*., 2001).

Recent studies of the human ortholog NVL2 identified other functions for nucleolar AAA+-factors beyond ribosome biogenesis (Fujiwara *et al.*, 2011). Through interaction with nucleolin, NVL2 is thought to supply energy for the TERT complex that is essential for maintenance of the telomere length and this opens a new role for the AAA+-family in cell aging (Fujiwara *et al*., 2011). To determine whether the loss of ts-TgNoAP1 affected telomere maintenance in *Toxoplasma*, we introduced a triple hemagglutinin tag (3xHA) into the *Toxoplasma* nucleolin gene (TGGT1_031630) in the F10^{Y984C} clone also expressing ts-TgNoAP1^{myc}. These experiments demonstrated that temperature had no effect on the localization or expression of the *Toxoplasma* nucleolin^{HA} protein, while as expected ts-TgNoAP1^{myc} levels declined upon high temperature shift in this dual-tagged strain (Figs. 7A-C). Importantly, the length of telomeres also did not show temperature-induced changes in any strain encoding either the wild type or mutant TgNoAP1 protein (Fig. 7D). Perhaps correlative to these results, we found that as the nucleolus fragmented during mitosis (and before ts-TgNoAP1^{myc} disappeared) nucleolin^{HA} and ts-TgNoAP1^{myc} proteins occupied different nucleolar fragments suggesting these factors associate with distinct nucleolar complexes (Fig. 7B, merge of nucleolin^{HA} and ts-TgNoAP1^{myc} staining in mitotic parasites at 34°C in the middle image panel).

TgNoAP1 associated with 90S pre-ribosome complexes

To help understand TgNoAP1 functions in *Toxoplasma*, we performed IP/LC-MS/MS on whole cell lysate and nuclear extracts of C6^{wt} clone expressing TgNoAP1^{myc} in comparison to parental RHΔ*ku80* lysates (Suvorova *et al.*, 2013). These analyses identified 108 proteins from nuclear extracts (NE) and 97 proteins from whole cell lysates (WHL) that were specifically enriched by TgNoAP1^{myc} immunoprecipitation. A total of 62 proteins were co-identified in both lysates (Dataset S2) with the largest group ribosomal proteins from both the small 40S and large 60S subunits. Importantly, we identified several factors involved in ribosomal RNA processing (Fig. 8) that correlates with the primary defect in the synthesis of 28S rRNA that was observed when ts-TgNoAP1 mutant parasites were incubated at high temperature (Fig. 6A and D). Critical post-transcriptional 2′-O-methylation and pseudouridine modification of unprocessed rRNA transcripts are catalyzed by conserved RNP complexes that are assembled on the box C/D and H/ACA snoRNAs (Fig. 8, diagrams of processing RNP complexes). The proteomic analysis revealed that TgNoAP1 may associate with the core components of the 2′-O-methylation complex (Nop56, Nop58, fibrillarin-domain protein and 15.5k) as well as several accessory factors coordinating assembly and translocation of snoRNP from nucleoplasm to nucleolus (RuvB1, RuvB2 and HSP70) (Fig. 8). Interestingly, the TgNoAP1^{myc} pulldowns did not enrich for components of the large 60S subunit maturation machinery (Dataset S2) (Kressler *et al*., 2012) nor did we uncover interactions with known protein partners of the yeast Rix7 or human NVL2, including the *Toxoplasma* orthologs of Wdr74 and nucleolin, which were evaluated earlier in this report (Fig. 7 and S4).

NIH-PA Author Manuscript

NIH-PA Author Manuscript

NIH-PA Author Manuscript

Discussion

Eukaryotic cell cycle checkpoints are control mechanisms that ensure each step in cell division occurs with high fidelity. By direct or indirect action, checkpoint regulators act as “traffic lights” at the cross roads of the major cell cycle pathways (Nasmyth, 2001). The traffic loading and timing are critical parameters for the smooth progression through the cell cycle stages. Such surveillance mechanisms lead to rapid uniform arrest of the affected population until the necessary requirement is fulfilled. *Toxoplasma* mutant 11-104A demonstrates many features consistent with a checkpoint defect. Once shifted to high temperature, mutant 11-104A4 rapidly arrests in a single phase of the present or next cell cycle. These results indicate that the parasite can progress into a second division cycle as long as the parasite was past the checkpoint mechanism triggered by the temperature shift. Of course the checkpoint remains active at high temperature trapping the parasite when it cycles around to the block in the next cell cycle. Consistent with the checkpoint scenario, mutant 11-104A4 populations arrested in the G1 period of the first or second cell cycle all within the timeframe of one full tachyzoite cell cycle (≤8 h). Based on cell biologic markers and specific transcriptome patterns at growth arrest, the cell cycle defect in mutant 11-104A4 affects a G1 “traffic stop”, which corrects the previous mis-categorization of this mutant as a DNA replication mutant (Gubbels *et al*., 2008a). The checkpoint that appears to be defective in the mutant 11-104A4 could be related to the previously described checkpoint revealed in G1 phase synchronization of tachyzoites by the drug pyrrolidine dithiocarbamate (Conde de Felipe *et al*., 2008). Pyrrolidine dithiocarbamate-inhibited parasites growth arrest with 1N genome content, and like mutant 11-104A4 cells at high temperature, these drug-treated parasites have a larger cell size consistent with the accumulation of cytosolic and nuclear material in the absence of commitment to chromosome replication. Genetic complementation of ts-strain 11-104A4 identified the mutation responsible for G1 arrest in a novel AAA+ ATPase protein, which implicated a cdc48-related mechanism as essential for parasite cell cycle progression.

AAA+ ATPases are factors that supply the energy of ATP hydrolysis to induce conformation changes in target substrates (for review see (Kressler *et al*., 2012, Duderstadt & Berger, 2008, White & Lauring, 2007)). Eukaryotes harbor many AAA+ factors where they participate in diverse functions including DNA replication, protein degradation and trafficking, and ribosome assembly. The genomes of apicomplexan parasites are also enriched for members of this gene family: the *Toxoplasma gondii* genome is predicted to encode 94 AAA+ factors (www.eupath.org). Many of the *Toxoplasma* AAA+-proteins show similarity to conserved helicases, proteases, ion transporters and atypical AAA+ proteins such as dyneins (Agrawal *et al.*, 2009). There is also a large group of AAA+ ATPases with unrecognized cellular function and among these are cdc48-related proteins including the essential AAA+ ATPase we have designated, TgNoAP1. TgNoAP1 protein is a nuclear factor exclusively localized to the parasite nucleolus where it is expressed in the G1 and S phases before disappearing at the onset of mitosis during normal fragmentation and reassembly of the nucleolus into daughter parasites. The major function of the nucleolus is to produce new ribosomes and the central production line from rRNA transcription and processing to ribosome subunit assembly is housed in this unusual subnuclear compartment (Thiry & Lafontaine, 2005). Three nucleolar AAA ATPases, Rix7/NVL2, Rea1/Midasin and Drg1/Afg2 are known to regulate the progression of ribosome assembly by promoting release of specific factors from pre-60S intermediates (Kressler *et al*., 2012). In human and yeast cells, NVL2 and Rix7, respectively, co-purify with early pre-60S ribosomal particles according to its first place in the 60S subunit assembly line (Gadal *et al*., 2001, Kressler *et al*., 2008) (Fig. 9). Consistent with this role, Rix7 defects cause the loss of 60S subunits and this has led to increased levels of 40S subunits and pre-cursor 35S rRNAs that encode unprocessed 28S rRNA (Gadal *et al*., 2001, Kressler *et al*., 2008). The evolutionary

NIH-PA Author Manuscript

NIH-PA Author Manuscript

NIH-PA Author Manuscript

similarity of TgNoAP1 to Rix7/NVL2 proteins, the exclusive localization of this factor to the parasite nucleolus, as well as its dynamic regulation during nucleolar remodeling in mitosis suggested early on that TgNoAP1 could be the apicomplexan equivalent of Rix7 and NVL2 ATPases. However, in trying to extend the resemblance to Rix7/NVL2 our studies of TgNoAP1 described here quickly diverged. For example, the loss of ts-TgNoAP1 at high temperature did not cause the expected build up of 35S precursor rRNA nor did we observe unusual polysome profiles that might indicate the presence of halfmer 40S-bound mRNA particles (Kressler *et al*., 2008). Likewise, the loss of ts-TgNoAP1 did not disrupt the expression or nucleolar localization of proteins known to interact with Rix7/NVL2 (i.e. nucleolin and the Nsa-1 ortholog Wdr74) nor were alternate functions affected such as telomere stability known to require NVL2 in human cells (Her & Chung, 2012). These counter experimental results led us to look at TgNoAp1 protein interactions and the proteomic results pointed towards a function for TgNoAP1 that is different than Rix7/NVL2. Enrichment of the small nucleolar RNP (snoRNP) components and associated complexes in these pulldowns suggest TgNoAP1 may have a role in regulating pre-rRNA processing and this role would be consistent with the primary decline of 28S rRNA in mutant 11-104A4. TgNoAP1 interactors are known to associate in snoRNPs, specifically the distinctive box C/D and H/ACA complexes that have primary functions in 2′-O-methylation and pseudouridine modification of the pre-rRNA (Fig. 8 and 9) (Gagnon *et al.*, 2010, Boisvert *et al.*, 2007, McKeegan *et al.*, 2009). Other identified TgNoAP1 interactions further support this new role for a cdc48-related factor. It has been shown that dynamic R2TP (Rvb1, Rvb2, Tah1, Pih1) complexes are involved in snoRNP assembly, and the timely translocation of snoRNP into nucleolus is required for the proper pre-rRNA processing (Fig. 8 and 9) (Boulon *et al.*, 2008, Huen *et al.*, 2010, Kakihara & Houry, 2012). A few subunits of the R2TP complex and accompanied HSP90/70 factors that assist these steps were found in TgNoAP1 precipitated complexes. Deciphering the TgNoAP1 mechanism is in an early phase, however, this study demonstrates that cdc48-related factors in these ancient eukaryotes have evolved to control other steps in ribosome biogenesis from the expected 60S subunit maturation/transport functions of Rix7/NVL2 to mechanisms that control rRNA synthesis prior to subunit assembly (Fig. 9).

The high-energy cost of ribosome biogenesis dominates the G1 phase of eukaryotic cells (Krastev & Buchholz, 2011, Warner, 1999) and as a consequence ribosome production is tightly linked to cell cycle progression. The cell cycle checkpoints that monitor this synthetic pathway operate by sensing changes in ribosome biogenesis prior to any significant loss of protein biosynthetic capacity (Bernstein *et al.*, 2007, Hutson *et al.*, 2010, Pestov *et al.*, 2001, Volarevic *et al.*, 2000). The cell cycle features of ts-TgNoAP1 loss in the mutant 11-104A also favor this type of regulatory framework. The immediate cell cycle arrest of 11-104A4 parasites is well before any significant loss of ribosome content nor is this arrest likely to be caused by general block to protein synthesis given the reversibility of this phenotype and abundant pool of the mRNA loaded polyribosomes over the first 8-10 h post-temperature shift. In yeast and animal cells, ribosome-sensing checkpoints appear to operate through the activity of classic retinoblastoma checkpoint mechanisms (Whi5 in yeast). Retinoblastoma protein in animal cells acts in a transcriptional network involving transcriptional factor E2F and cyclin D and E (Qu *et al.*, 2003), while in yeast the SBF/MBF transcription complexes and cyclins CLN1-3 are the key players (Bahler, 2005). This linkage may be specifically bridged by cell cycle checkpoint factors that have independent functions in both processes. For example, the ARF tumor suppressor is a nucleolar protein that inhibits rRNA processing and also activates p53 (Sugimoto *et al.*, 2003), which in turn prevents the phosphorylation of retinoblastoma through induction of the G1 cyclin regulator, p21 (Harper *et al.*, 1993). Other nucleolar factors required for ribosome biogenesis in mammalian cells may also provide a link to the cell cycle through p53 including constituents of the PeBoW complex involved in 60S subunit synthesis (Holzel *et al.*, 2005) and

NIH-PA Author Manuscript

NIH-PA Author Manuscript

NIH-PA Author Manuscript

ribosomal proteins (L5, L11, L23) that interact with the E3 ligase Hdm2 responsible for regulating p53 stability (Holzel *et al.*, 2010). How apicomplexan parasites regulate the complex biosynthetic machinery in G1 including ribosome biogenesis is not understood as the specific nodes in the retinoblastoma associated mechanisms including retinoblastoma protein itself are absent (Behnke *et al.*, 2010). The discovery here of the molecular chaperone TgNoAP1 and its potential interaction with snoRNP machinery provides a new avenue to investigate how ribosome biogenesis is regulated and to begin uncovering the molecular basis of G1 control in these parasites. Other proteins of interest from the TgNoAP1 proteomics is a group of histones H2.Z and H4 that are known to occupy promoters of the silent genes (Svotelis *et al.*, 2009, Petter *et al.*, 2011) and unique apicomplexan serine-threonine kinase that has a pronounced cell cycle expression pattern (TGME49_031070). Understanding G1-linked mechanisms in these pathogens has new urgency, as it is now clear cycling between replication and dormancy in G1/G0 contributes to drug resistance particularly in the emergence of artemisinin resistance in strains of *Plasmodium falciparum* (Tucker *et al*., 2012, Teuscher *et al*., 2012). For instance, recent mapping of the major loci linked to the chloroquinine resistance in *P. falciparum* revealed inheritance of the several cell cycle markers, including core snoRNP factor RPL7Ae that correlates with increased proliferation rate and shortening of the G1 phase (Reilly Ayala *et al.*, 2010). Therefore, it is reasonable to hypothesize that the *de novo* production of ribosomes that is dependent of RPL7Ae is one of the checkpoints where the critical G1/G0 decision is made and the factors of TgNoAP1 family represent one of the nodes controlling this mechanism. Exploiting the differences observed in pathways that control Apicomplexa cell cycle progression, like the G1 mechanism involving TgNoAP1, suggest that dissecting these mechanisms could lead to new drugs that target specific cell cycle checkpoint mechanisms.

Experimental procedures

Parasite cell culture

Parasites were grown in human foreskin fibroblasts (HFF) as described (Roos *et al.*, 1994). All transgenic and mutant parasite lines are derivatives of the RHΔ*hxgprt* parasite strain. Temperature sensitive clone 11-104A4 was obtained by chemical mutagenesis of the RHΔ*hxgprt* strain (Gubbels *et al*., 2008a). Growth measurements were obtained using parasites pre-synchronized by limited invasion as previously described (Gaji *et al.*, 2011, Suvorova *et al*., 2012). Parasite vacuoles in the infected plates were evaluated over various time periods with average vacuole sizes determined at each time point from 50-100 randomly selected vacuoles.

Immunofluorescence

Confluent HFF cultures on the glass coverslips were infected with parasites for the indicated time. Infected monolayers were fixed, permeabilized and incubated with antibody as previously described (Suvorova *et al*., 2012). The following primary antibodies were used at 1:1000 dilution: mouse monoclonal αMyc (Santa Cruz Biotechnology, Santa Cruz, CA), αAtrx1 and αROP7 (apicoplast and rhoptry stains, respectfully, kindly provided by Dr. Peter Bradley, UCLA, Los Angeles, CA), αTgNF3 (nucleolus stain, kindly provided by Dr. Stanislas Tomavo, University Lille Nord de France, Lille, France), αH fibrillarin (nucleolus stain) (Reimer *et al.*, 1987), rat monoclonal αHA (Roche), rabbit polyclonal αHuman centrin 1 (centrosome stain, Suvorova and White, unpublished), αMORN1 (spindle pole and basal complex stains, kindly provided by Dr. Mark-Jan Gubbels, Boston College, MA) and αIMC1 (parasite shape and internal daughter bud stains, kindly provided by Dr. Gary Ward, University of Vermont, VT). Serum raised against the conserved human centrin 1 was previously shown to cross-react with the *Toxoplasma* centrin ortholog (Suvorova *et al*.,

NIH-PA Author Manuscript

NIH-PA Author Manuscript

NIH-PA Author Manuscript

2012). All Alexa-conjugated secondary antibodies (Molecular Probes, Life Technologies) were used at dilution 1:1000. Coverslips were mounted with Aquamount (Thermo Scientific), dried overnight at 4°C, and viewed on Zeiss Axiovert Microscope equipped with 100x objective. Images were processed in Adobe Photoshop CS v4.0 using linear adjustment for all channels.

Genetic rescue and secondary complementation

Mutant 11-104A4 was complemented using the ToxoSuperCos cosmid genomic library as previously described (Gubbels *et al*., 2008a, Suvorova *et al*., 2012). Mutant parasites were transfected with cosmid library DNA (50 μg DNA/5 × 10^7 parasites/transfection) in twenty independent electroporations. After two consecutive selections at 40°C, parasites were selected by the combination of high temperature and 1 μM pyrimethamine. Double resistant populations were passed four times before genomic DNA was isolated for marker-rescue (Gubbels *et al*., 2008a). To identify the complementing locus in *Toxoplasma* chromosomes, rescued genomic inserts were sequenced using a T3 primer and the sequences mapped to the *Toxoplasma* genome (ToxoDB: http://www.toxodb.org/toxo/).

To resolve the contribution of individual genes in the recovered locus, we transformed the mutant 11-104A4 with individual cosmids from a cosmid collection mapped to the *Toxoplasma* genome (toxomap.wustl.edu/cosmid.html). For direct complementation with DNA fragments, the TGGT1_117040 gene locus was amplified from genomic DNA isolated from the parental strain RHΔ*hxgprt* or the mutant 11-104A4 using forward primer TgNoAP1_FOR located at −1000bp in the 5′ UTR and reverse primer TgNoAP1_REV located 12bp downstream of the stop codon of TGGT1_117040 gene (Table S1). *Specific cosmids* (TOXOV53 and PSBLD53) or PCR fragments were transfected into 1×10^7 parasites using 6-10 μg of purified DNA. To quantify genetic rescue, established drug-resistant populations were tested for growth at the high temperature by standard plaque assay performed in triplicate (Striepen *et al*., 2007).

To investigate the ATPase activity of TgNoAP1 conserved lysine residues K495 and K992 in the two Walker A motifs were mutated to alanines by site-directed mutagenesis. Individual target mutations were sequentially introduced into TgNoAP1 cDNA inserted in pCR4Blunt TOPO vector (Invitrogen) by inverse PCR. PCR fragments of the wild type, ts-allele and the dual mutant K495A/K992A TgNoAP1 were amplified from the pCR4Blunt TOPO vector using T3 and T7 primers. Mutant 11-104A4 parasites were transfected with 5μg of DNA per 2×10^7 cells and evaluated for growth at 40°C by plaque assay.

Generation of transgenic tachyzoite strains

Epitope tagging of proteins by gene knock-in—A new strain expressing the ts-TgNoAP1 allele was generated in the RHΔ*ku80* strain (clone $F10^{Y984C}$ expressing ts-$TgNoAP1^{myc}$). To reintroduce the Y984C mutation into a new genomic background, we PCR amplified a 3,163bp DNA fragment from mutant 11-104A4 that includes the 3′ end of the TGGT1_117040 (ts-TgNoAP1) using primers LIC-TgNoAP1_FOR and LIC-TgNoAP1_REV (Table S1). In parallel, we also amplified a genomic fragment from the wild type TGGT1_117040 locus in the RHΔ*ku80* to generate 3xmyc tagged native $TgNoAP1^{myc}$ in the transgenic strain $C6^{wt}$. The PCR products were cloned into pLIC-myc_{3X}/*dhfr*-HXGPRT vector and resulting constructs introduced in RHΔ*ku80* strain deficient in non-homologous recombination (Huynh & Carruthers, 2009). Expression of the tagged proteins was verified by IFA.

Epitope tagging of *Toxoplasma* nucleolin (TGGT1_031630) with a triple copy of the HA tag was also accomplished by genetic knock-in. PCR DNA fragments encompassing the 3′-end

NIH-PA Author Manuscript

NIH-PA Author Manuscript

NIH-PA Author Manuscript

of the nucleolin gene were used to construct the plasmid, pLIC-TgNucleolin-HA_{3X}/*dhfr*-DHFR-TS (see Table S1 for primers designs) and the construct electroporated into the clone $F10^{Y984C}$ that expresses ts-$TgNoAP1^{myc}$ protein. The double-tagged transgenic line was established under pyrimethamine selection and expression of the fusion proteins was verified by IFA.

Ectopic expression of epitope tagged proteins—The coding sequences of TgRPL36 (TGGT1_052600) and TgWdr74 (TGGT1_080560) were amplified from a parental RHΔ*hxgprt* cDNA library (see Table S1 for primers designs) and the DNA fragments cloned into the pDEST_gra-myc_{3X}/sag-HXGPRT vector by recombination (Gateway cloning, Life Technologies), which fuses a triple myc tag to the C-terminus of each protein. Plasmid constructs were introduced in the parental RHΔ*hxgprt* strain and mutant 11-104A4, and selected in the medium with mycophenolic acid and xanthine. Established clones were analyzed by immunofluorescent microscopy, western blot analysis and tested for growth at 40°C.

Western blot analysis

Purified parasites were washed in PBS and collected by centrifugation. Total lysates were obtained by mixing with Leammli loading dye, heated at 95°C for 10 min, and briefly sonicated. After separation on the SDS-PAGE gels, proteins were transferred onto nitrocellulose membrane and probed with monoclonal antibodies against Myc-epitope (mouse 9E10, Santa Cruz Biotechnology) and α-tubulin (mouse 12G10, kindly provided by Jacek Gaertig, University of Georgia), and HA-epitope (rat 3F10, Roche Applied Sciences). After incubation with secondary HRP-conjugated anti-mouse or anti-rat antibodies, proteins were visualized by enhanced chemiluminescence detection (PerkinElmer).

Southern Blot analysis of telomeric regions

The telomere probe was generated from CpGR254 plasmid described in (Liu *et al.*, 1998). Briefly, plasmid DNA containing the apicomplexan telomere repeat sequence first identified in *Cryptosporidium parvum* was digested with KpnI/SacI, the insert purified and the DNA labeled with biotin using the North2South Biotin Random Prime Labeling Kit (Thermo Scientific). Genomic DNA was purified from parasites incubated at 34°C or 40°C. The resulting gDNA was digested to completion using PstI and subjected to Southern Blot analysis as previously described (Liu *et al*., 1998, Kimura *et al.*, 2010) with minor changes. Briefly, gDNA PstI fragments were resolved on a 1% agarose gel and transferred overnight to a nylon membrane (Thermo Scientific). Following transfer, DNA was cross-linked to the membrane (UV Stratalinker 1800, auto setting), hybridized with the biotinylated telomere probe overnight, and bound DNA detected using the North2South Chemiluminescent Hybridization and Detection kit (Thermo Scientific) according to manufacturer protocols.

Phylogenetic analysis of ATPase orthologs

Orthologs of TgNoAP1 (TGGT1_117040) were identified by BLAST and aligned by ClustalW2. Evolutionary analyses were conducted in Phylogeny.fr (Dereeper *et al.*, 2010). All positions containing gaps and missing data were eliminated from aligned amino acid sequences, which resulted in a total of 212 positions in the final dataset. The bootstrap consensus tree inferred from 500 replicates represents the evolutionary history of the TgNoAP1 family analyzed by the Maximum Likelihood method based on the WAG substitution model (Dereeper *et al*., 2008). Analyzed species and corresponding gene ID of the cdc48-related family proteins: *Toxoplasma gondii* (TGGT1_117040), *Babesia bovis* (BBOV_IV011460), *Cryptosporidium parvum* (cgd5_2010), *Plasmodium falciparum* (PF3D7_0814300), *Saccharomyces cerevisiae* (NP_013066.1) and *Homo sapiens*

NIH-PA Author Manuscript

NIH-PA Author Manuscript

NIH-PA Author Manuscript

(NP_001230075.1). Analyzed species and corresponding gene ID of the cdc48 family proteins: *Toxoplasma gondii* (TGME49_273090) cytoplasmic cdc48, *Toxoplasma gondii* (TGME49_321640) apicoplast cdc48, *Saccharomyces cerevisiae* (NP_010157.1) and *Homo sapiens* (NP_009057.1).

RNA isolation and microarray analysis

Mutant 11-104A4 cells were incubated at 34°C for 16 h, and then were either shifted to 40°C or left at 34°C for another 32 h. Similarly, a drug resistant population of the mutant 11-104A4 complemented with TOXOV53 cosmid was grown at 40°C. All parasite samples were filtered through 3μm membrane, pelleted, washed with cold PBS and stored at −80°C. RNA was extracted with the RNeasy kit (Qiagen) and cRNA was produced using the Affymetrix One-Cycle Kit (Affymetrix). RNA quality was assessed using the Agilent Bioanalyzer 2100 (Agilent Technologies) and fragmented cRNA (5μg) was hybridized to the *Toxoplasma gondii* Affymetrix microarray according to standard hybridization protocols (ToxoGeneChip: http://ancillary.toxodb.org/docs/Array-Tutorial.html). Two hybridizations were done for each sample type and all data were deposited at NCBI GEO (GSE43784). Hybridization data was preprocessed with Robust Multi-array Average (RMA) and normalized using per chip and per gene median polishing and analyzed using the software package GeneSpring GX (Agilent Technologies). An ANOVA or t-test were run in order to identify genes with significantly greater than random variation in RNA abundance across the data grouped by either temperature or mutant type. Variances were calculated using cross-gene error model, with a p-value cutoff 0.1, and multiple testing correction: Benjamini and Hochberg False Discovery Rate. This restriction tested 8,131 probe sets. Please see Dataset S1 in supplemental information for full gene lists.

Polyribosome fractionation

Parental RHΔ*hxgprt* strain and mutant 11-104A4 parasites expressing TgRPL36^{myc} were grown at 34°C for 27-33h (parent-mutant, respectively) and then shifted to 40°C for 10 h. Cycloheximide (100μg/ml) was added to the cultures 10 min prior collection. To obtain cytosolic extracts, 5×10^8 purified parasites were lysed in the 20mM Tris buffer pH 7.4 containing 10mM NaCl, 3 mM MgCl, 1% Triton X-100, 1mg/ml heparin, 7% sucrose, 100μg/ml cycloheximide and protease inhibitor cocktail (Thermo Scientific) for 30 min on ice. To obtain cytoplasmic lysates nuclei and unlysed cells were removed by centrifugation at 21,000xg, 15 min, 4°C. Cytoplasmic lysates were supplemented with 100mM NaCl and loaded onto 15%-40% sucrose step gradient over a 0.5ml 70% sucrose cushion. The gradient was run for 3 h at 30,000 rpm at 4°C in a SureSpin 630 rotor (Thermo Scientific). Absorbance at 254nm was measured in sucrose gradient fractions (26 total, 0.5ml). For western analysis the two adjoining fractions were pooled together (13 samples) and a 1/5th sample was taken to precipitate proteins with trichloric acid. RNA was extracted from the remaining 4/5th gradient fractions with phenol/chlorophorm and precipitated with ethanol. RNA from the last 4 fractions (9 to 13) were pooled together prior to the run on the Agilent Bioanalyzer (Agilent Technologies).

Immunoprecipitation and protein chromatography coupled mass spectrometry

Parental RHΔ*ku80* and C6^{wt} parasites expressing TgNoAP1^{myc} were used in proteomics studies. Whole cell lysates and nuclear extracts were obtained from 2×10^9 cells and subjected to Immunoprecipitation as previously described (Suvorova *et al*., 2013). Protein extracts were rotated overnight at 4°C with magnetic beads (MBL International, MA) containing pre-bound monoclonal anti-Myc antibody (Santa Cruz Biotechnology). Washed beads were heated for 5 min at 95°C in 50μl Laemmli sample buffer to elute bound proteins. Precipitated complexes were separated by SDS-PAGE (Any kD precast polyacrylamide gel;

NIH-PA Author Manuscript

NIH-PA Author Manuscript

NIH-PA Author Manuscript

Bio-Rad) and stained with Coomassie Blue (GelCode Blue Stain Reagent, Pierce). Each sample lane was cut into 24 slices and separately analyzed by liquid chromatography coupled to mass-spectrometry as described (Suvorova *et al*., 2013). Briefly, proteins reduced and alkylated with TCEP and iodoacetamide were digested with trypsin, and run sequentially on Acclaim PepMap C18 Nanotrap column and PepMap RSLC C18 column (Dionex Corp). Raw LC-MS/MS data was collected using Proteome Discoverer 1.2 (Thermo Scientific) and proteins were searched in the Toxo_Human Combined database using in-house Mascot Protein Search engine (Matrix Science). Final list was generated in the Scaffold 3.5.1 (Proteome Software) with following filters: 99% minimum protein probability, minimum number peptides of 2 and 95% peptide probability.

Supplementary Material

Refer to Web version on PubMed Central for supplementary material.

Acknowledgments

This work was supported by grants from the National Institutes of Health to MWW (R01-AI077662 and R01-AI089885). *T. gondii* genomic and/or cDNA sequence data were accessed via http://ToxoDB.org. The authors would like to thank Dr. Olivier Lucas (University of South Florida, Tampa FL), Margaret M. Lehmann and Kate McInnerney (Montana State University, Bozeman, MT) for technical assistance. We are indebted to Myrasol Callaway (Albert Einstein College of Medicine, Bronx, NY) for help with proteomics supported by NIH shared instrumentation grants (1S10RR019352, 1S10RR021056).

References

Agrawal S, van Dooren GG, Beatty WL, Striepen B. Genetic evidence that an endosymbiont-derived endoplasmic reticulum-associated protein degradation (ERAD) system functions in import of apicoplast proteins. J Biol Chem. 2009; 284:33683–33691. [PubMed: 19808683]

Bahler J. Cell-cycle control of gene expression in budding and fission yeast. Annu Rev Genet. 2005; 39:69–94. [PubMed: 16285853]

Behnke MS, Wootton JC, Lehmann MM, Radke JB, Lucas O, Nawas J, Sibley LD, White MW. Coordinated progression through two subtranscriptomes underlies the tachyzoite cycle of Toxoplasma gondii. PLoS One. 2010; 5:e12354. [PubMed: 20865045]

Bernstein KA, Bleichert F, Bean JM, Cross FR, Baserga SJ. Ribosome biogenesis is sensed at the Start cell cycle checkpoint. Mol Biol Cell. 2007; 18:953–964. [PubMed: 17192414]

Boisvert FM, van Koningsbruggen S, Navascues J, Lamond AI. The multifunctional nucleolus. Nat Rev Mol Cell Biol. 2007; 8:574–585. [PubMed: 17519961]

Boulon S, Marmier-Gourrier N, Pradet-Balade B, Wurth L, Verheggen C, Jady BE, Rothe B, Pescia C, Robert MC, Kiss T, Bardoni B, Krol A, Branlant C, Allmang C, Bertrand E, Charpentier B. The Hsp90 chaperone controls the biogenesis of L7Ae RNPs through conserved machinery. J Cell Biol. 2008; 180:579–595. [PubMed: 18268104]

Bozdech Z, Llinas M, Pulliam BL, Wong ED, Zhu J, DeRisi JL. The transcriptome of the intraerythrocytic developmental cycle of Plasmodium falciparum. PLoS Biol. 2003; 1:E5. [PubMed: 12929205]

Briggs LC, Baldwin GS, Miyata N, Kondo H, Zhang X, Freemont PS. Analysis of nucleotide binding to P97 reveals the properties of a tandem AAA hexameric ATPase. J Biol Chem. 2008; 283:13745–13752. [PubMed: 18332143]

Conde de Felipe MM, Lehmann MM, Jerome ME, White MW. Inhibition of Toxoplasma gondii growth by pyrrolidine dithiocarbamate is cell cycle specific and leads to population synchronization. Mol Biochem Parasitol. 2008; 157:22–31. [PubMed: 17976834]

Dereeper A, Audic S, Claverie JM, Blanc G. BLAST-EXPLORER helps you building datasets for phylogenetic analysis. BMC Evol Biol. 2010; 10:8. [PubMed: 20067610]

NIH-PA Author Manuscript

NIH-PA Author Manuscript

NIH-PA Author Manuscript

Dereeper A, Guignon V, Blanc G, Audic S, Buffet S, Chevenet F, Dufayard JF, Guindon S, Lefort V, Lescot M, Claverie JM, Gascuel O. Phylogeny.fr: robust phylogenetic analysis for the non-specialist. Nucleic Acids Res. 2008; 36:W465–469. [PubMed: 18424797]

Duderstadt KE, Berger JM. AAA+ ATPases in the initiation of DNA replication. Crit Rev Biochem Mol Biol. 2008; 43:163–187. [PubMed: 18568846]

Fujiwara Y, Fujiwara K, Goda N, Iwaya N, Tenno T, Shirakawa M, Hiroaki H. Structure and function of the N-terminal nucleolin binding domain of nuclear valosin-containing protein-like 2 (NVL2) harboring a nucleolar localization signal. J Biol Chem. 2011; 286:21732–21741. [PubMed: 21474449]

Gadal O, Strauss D, Braspenning J, Hoepfner D, Petfalski E, Philippsen P, Tollervey D, Hurt E. A nuclear AAA-type ATPase (Rix7p) is required for biogenesis and nuclear export of 60S ribosomal subunits. Embo J. 2001; 20:3695–3704. [PubMed: 11447111]

Gagnon KT, Zhang X, Qu G, Biswas S, Suryadi J, Brown BA 2nd, Maxwell ES. Signature amino acids enable the archaeal L7Ae box C/D RNP core protein to recognize and bind the K-loop RNA motif. Rna. 2010; 16:79–90. [PubMed: 19926724]

Gaji RY, Behnke MS, Lehmann MM, White MW, Carruthers VB. Cell cycle-dependent, intercellular transmission of Toxoplasma gondii is accompanied by marked changes in parasite gene expression. Mol Microbiol. 2011; 79:192–204. [PubMed: 21166903]

Gubbels MJ, Lehmann M, Muthalagi M, Jerome ME, Brooks CF, Szatanek T, Flynn J, Parrot B, Radke J, Striepen B, White MW. Forward genetic analysis of the apicomplexan cell division cycle in Toxoplasma gondii. PLoS Pathog. 2008a; 4:e36. [PubMed: 18282098]

Gubbels MJ, Vaishnava S, Boot N, Dubremetz JF, Striepen B. A MORN-repeat protein is a dynamic component of the Toxoplasma gondii cell division apparatus. J Cell Sci. 2006; 119:2236–2245. [PubMed: 16684814]

Gubbels MJ, White M, Szatanek T. The cell cycle and Toxoplasma gondii cell division: tightly knit or loosely stitched? International journal for parasitology. 2008b; 38:1343–1358. [PubMed: 18703066]

Harper JW, Adami GR, Wei N, Keyomarsi K, Elledge SJ. The p21 Cdk-interacting protein Cip1 is a potent inhibitor of G1 cyclin-dependent kinases. Cell. 1993; 75:805–816. [PubMed: 8242751]

Her J, Chung IK. The AAA-ATPase NVL2 is a telomerase component essential for holoenzyme assembly. Biochem Biophys Res Commun. 2012; 417:1086–1092. [PubMed: 22226966]

Hernandez-Verdun D. Assembly and disassembly of the nucleolus during the cell cycle. Nucleus. 2011; 2:189–194. [PubMed: 21818412]

Holzel M, Burger K, Muhl B, Orban M, Kellner M, Eick D. The tumor suppressor p53 connects ribosome biogenesis to cell cycle control: a double-edged sword. Oncotarget. 2010; 1:43–47. [PubMed: 21293052]

Holzel M, Rohrmoser M, Schlee M, Grimm T, Harasim T, Malamoussi A, Gruber-Eber A, Kremmer E, Hiddemann W, Bornkamm GW, Eick D. Mammalian WDR12 is a novel member of the Pes1-Bop1 complex and is required for ribosome biogenesis and cell proliferation. J Cell Biol. 2005; 170:367–378. [PubMed: 16043514]

Huen J, Kakihara Y, Ugwu F, Cheung KL, Ortega J, Houry WA. Rvb1-Rvb2: essential ATP-dependent helicases for critical complexes. Biochem Cell Biol. 2010; 88:29–40. [PubMed: 20130677]

Hutson SL, Mui E, Kinsley K, Witola WH, Behnke MS, El Bissati K, Muench SP, Rohrman B, Liu SR, Wollmann R, Ogata Y, Sarkeshik A, Yates JR 3rd, McLeod R. T. gondii RP promoters, & knockdown reveal molecular pathways associated with proliferation and cell-cycle arrest. PLoS One. 2010; 5:e14057. [PubMed: 21124925]

Huynh MH, Carruthers VB. Tagging of endogenous genes in a Toxoplasma gondii strain lacking Ku80. Eukaryot Cell. 2009; 8:530–539. [PubMed: 19218426]

Kakihara Y, Houry WA. The R2TP complex: discovery and functions. Biochim Biophys Acta. 2012; 1823:101–107. [PubMed: 21925213]

Kimura M, Stone RC, Hunt SC, Skurnick J, Lu X, Cao X, Harley CB, Aviv A. Measurement of telomere length by the Southern blot analysis of terminal restriction fragment lengths. Nature protocols. 2010; 5:1596–1607.

NIH-PA Author Manuscript

NIH-PA Author Manuscript

NIH-PA Author Manuscript

Krastev DB, Buchholz F. Ribosome biogenesis and p53: who is regulating whom? Cell Cycle. 2011; 10:3417–3418. [PubMed: 22067651]

Kressler D, Hurt E, Bergler H, Bassler J. The power of AAA-ATPases on the road of pre-60S ribosome maturation--molecular machines that strip pre-ribosomal particles. Biochim Biophys Acta. 2012; 1823:92–100. [PubMed: 21763358]

Kressler D, Roser D, Pertschy B, Hurt E. The AAA ATPase Rix7 powers progression of ribosome biogenesis by stripping Nsa1 from pre-60S particles. J Cell Biol. 2008; 181:935–944. [PubMed: 18559667]

Liu C, Schroeder AA, Kapur V, Abrahamsen MS. Telomeric sequences of Cryptosporidium parvum. Mol Biochem Parasitol. 1998; 94:291–296. [PubMed: 9747979]

McKeegan KS, Debieux CM, Watkins NJ. Evidence that the AAA+ proteins TIP48 and TIP49 bridge interactions between 15.5K and the related NOP56 and NOP58 proteins during box C/D snoRNP biogenesis. Mol Cell Biol. 2009; 29:4971–4981. [PubMed: 19620283]

Nagahama M, Hara Y, Seki A, Yamazoe T, Kawate Y, Shinohara T, Hatsuzawa K, Tani K, Tagaya M. NVL2 is a nucleolar AAA-ATPase that interacts with ribosomal protein L5 through its nucleolar localization sequence. Mol Biol Cell. 2004; 15:5712–5723. [PubMed: 15469983]

Nagahama M, Yamazoe T, Hara Y, Tani K, Tsuji A, Tagaya M. The AAA-ATPase NVL2 is a component of pre-ribosomal particles that interacts with the DExD/H-box RNA helicase DOB1. Biochem Biophys Res Commun. 2006; 346:1075–1082. [PubMed: 16782053]

Nasmyth K. A prize for proliferation. Cell. 2001; 107:689–701. [PubMed: 11747804]

Niwa H, Ewens CA, Tsang C, Yeung HO, Zhang X, Freemont PS. The role of the N-domain in the ATPase activity of the mammalian AAA ATPase p97/VCP. J Biol Chem. 2012; 287:8561–8570. [PubMed: 22270372]

Olguin-Lamas A, Madec E, Hovasse A, Werkmeister E, Callebaut I, Slomianny C, Delhaye S, Mouveaux T, Schaeffer-Reiss C, Van Dorsselaer A, Tomavo S. A novel Toxoplasma gondii nuclear factor TgNF3 is a dynamic chromatin-associated component, modulator of nucleolar architecture and parasite virulence. PLoS Pathog. 2011; 7:e1001328. [PubMed: 21483487]

Pestov DG, Strezoska Z, Lau LF. Evidence of p53-dependent cross-talk between ribosome biogenesis and the cell cycle: effects of nucleolar protein Bop1 on G(1)/S transition. Mol Cell Biol. 2001; 21:4246–4255. [PubMed: 11390653]

Petter M, Lee CC, Byrne TJ, Boysen KE, Volz J, Ralph SA, Cowman AF, Brown GV, Duffy MF. Expression of P. falciparum var genes involves exchange of the histone variant H2A.Z at the promoter. PLoS Pathog. 2011; 7:e1001292. [PubMed: 21379342]

Qu Z, Weiss JN, MacLellan WR. Regulation of the mammalian cell cycle: a model of the G1-to-S transition. Am J Physiol Cell Physiol. 2003; 284:C349–364. [PubMed: 12388094]

Radke JR, Striepen B, Guerini MN, Jerome ME, Roos DS, White MW. Defining the cell cycle for the tachyzoite stage of Toxoplasma gondii. Mol Biochem Parasitol. 2001; 115:165–175. [PubMed: 11420103]

Reilly Ayala HB, Wacker MA, Siwo G, Ferdig MT. Quantitative trait loci mapping reveals candidate pathways regulating cell cycle duration in Plasmodium falciparum. BMC Genomics. 2010; 11:577. [PubMed: 20955606]

Reimer G, Pollard KM, Penning CA, Ochs RL, Lischwe MA, Busch H, Tan EM. Monoclonal autoantibody from a (New Zealand black × New Zealand white)F1 mouse and some human scleroderma sera target an Mr 34,000 nucleolar protein of the U3 RNP particle. Arthritis Rheum. 1987; 30:793–800. [PubMed: 2441711]

Roos DS, Donald RG, Morrissette NS, Moulton AL. Molecular tools for genetic dissection of the protozoan parasite Toxoplasma gondii. Methods Cell Biol. 1994; 45:27–63. [PubMed: 7707991]

Rouiller I, DeLaBarre B, May AP, Weis WI, Brunger AT, Milligan RA, Wilson-Kubalek EM. Conformational changes of the multifunction p97 AAA ATPase during its ATPase cycle. Nat Struct Biol. 2002; 9:950–957. [PubMed: 12434150]

Sanz E, Yang L, Su T, Morris DR, McKnight GS, Amieux PS. Cell-type-specific isolation of ribosome-associated mRNA from complex tissues. Proc Natl Acad Sci U S A. 2009; 106:13939–13944. [PubMed: 19666516]

NIH-PA Author Manuscript

NIH-PA Author Manuscript

NIH-PA Author Manuscript

Striepen B, Jordan CN, Reiff S, van Dooren GG. Building the perfect parasite: cell division in apicomplexa. PLoS Pathog. 2007; 3:e78. [PubMed: 17604449]

Sugimoto M, Kuo ML, Roussel MF, Sherr CJ. Nucleolar Arf tumor suppressor inhibits ribosomal RNA processing. Mol Cell. 2003; 11:415–424. [PubMed: 12620229]

Suvorova ES, Croken M, Kratzer S, Ting LM, de Felipe MC, Balu B, Markillie ML, Weiss LM, Kim K, White MW. Discovery of a splicing regulator required for cell cycle progression. PLoS Genet. 2013; 9:e1003305. [PubMed: 23437009]

Suvorova ES, Lehmann MM, Kratzer S, White MW. Nuclear actin-related protein is required for chromosome segregation in Toxoplasma gondii. Mol Biochem Parasitol. 2012; 181:7–16. [PubMed: 21963440]

Svotelis A, Gevry N, Gaudreau L. Regulation of gene expression and cellular proliferation by histone H2A.Z. Biochem Cell Biol. 2009; 87:179–188. [PubMed: 19234533]

Teuscher F, Chen N, Kyle DE, Gatton ML, Cheng Q. Phenotypic changes in artemisinin-resistant Plasmodium falciparum lines in vitro: evidence for decreased sensitivity to dormancy and growth inhibition. Antimicrob Agents Chemother. 2012; 56:428–431. [PubMed: 21986828]

Thiry M, Lafontaine DL. Birth of a nucleolus: the evolution of nucleolar compartments. Trends Cell Biol. 2005; 15:194–199. [PubMed: 15817375]

Tucker MS, Mutka T, Sparks K, Patel J, Kyle DE. Phenotypic and genotypic analysis of in vitro-selected artemisinin-resistant progeny of Plasmodium falciparum. Antimicrob Agents Chemother. 2012; 56:302–314. [PubMed: 22083467]

Volarevic S, Stewart MJ, Ledermann B, Zilberman F, Terracciano L, Montini E, Grompe M, Kozma SC, Thomas G. Proliferation, but not growth, blocked by conditional deletion of 40S ribosomal protein S6. Science. 2000; 288:2045–2047. [PubMed: 10856218]

Warner JR. The economics of ribosome biosynthesis in yeast. Trends Biochem Sci. 1999; 24:437–440. [PubMed: 10542411]

White MW, Kameji T, Pegg AE, Morris DR. Increased efficiency of translation of ornithine decarboxylase mRNA in mitogen-activated lymphocytes. Eur J Biochem. 1987; 170:87–92. [PubMed: 3691536]

White SR, Lauring B. AAA+ ATPases: achieving diversity of function with conserved machinery. Traffic. 2007; 8:1657–1667. [PubMed: 17897320]

NIH-PA Author Manuscript
NIH-PA Author Manuscript
NIH-PA Author Manuscript

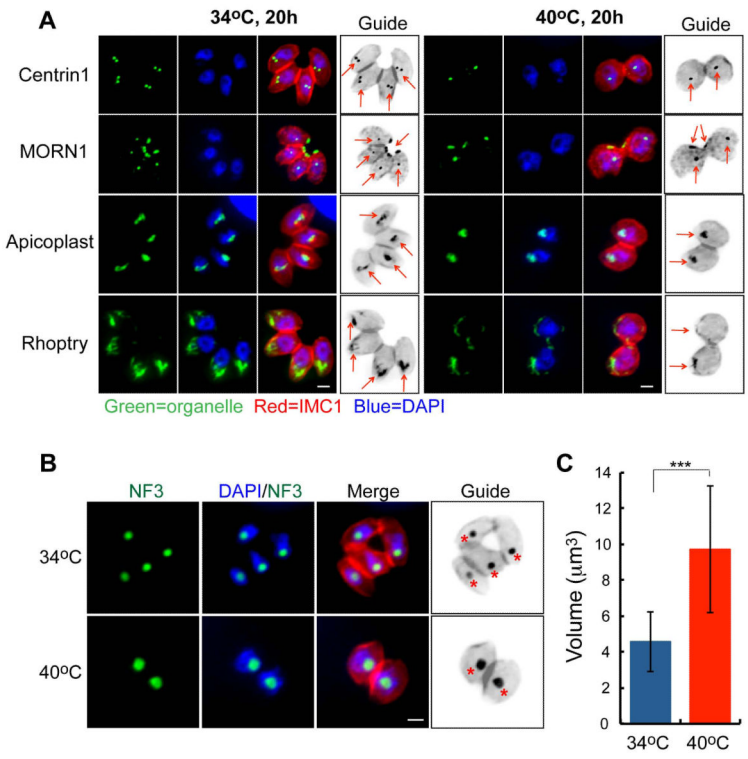

Figure 1. Mutant 11-104A4 conditionally arrests in the G1 phase of the tachyzoite cell cycle

(A) Mutant parasites were grown for 20 h at 34°C (left image panels) or 40°C (right image panels), fixed, and co-stained with a series of organellar antibodies (all green); αHuman-centrin1 (centrosomes), αMORN1 (spindle pole and basal complex), αAtrx1 (Apicoplast) and αROP7 (Rhoptry). Staining for the inner-membrane-complex protein 1 (IMC1, red) indicates parasite size and the presence of internal daughters, and DAPI (blue) was utilized to visualize nuclear chromosomes. Arrows in the marker guide panel, which is a B&W inverse of the merged red and green staining, indicates organelle location in the each image series. Staining with αHuman centrin1 antibodies demonstrates that a single centrosome predominates in mutant parasites at 40°C in comparison to duplicated centrosomes in the 34°C images. The spindle protein, MORN1, also shows a single structure internally as well as the post-cytokinesis basal body that resides at the extreme posterior end of each parasite. Scale bar = 2μm. **(B)** Enlargement of nuclear compartments appeared to be partially responsible for the temperature-induced increase of mutant 11-104A4 parasite size. This observation was confirmed by staining mutant parasites grown for 24 h at 34°C or 40°C with antibodies to the nucleolar factor, TgNF3 (green) (Olguin-Lamas *et al*., 2011). Co-staining with DAPI and αIMC1 antibody was used to visualize the nuclear chromatin compartment (blue) and parasite shape (red), respectively. A marker guide reference labels the nucleolus with a star. Scale bar = 2μm. **(C)** The nuclear volume was quantified in mutant populations at two growth temperatures (24 h at 34°C or 40°C). The nuclear diameter was estimated in the DAPI images of fifty randomly selected cells using AxioVision software. Calculated nuclear volumes and statistical variations between samples are shown in the graph (***, $p < 0.005$).

NIH-PA Author Manuscript
NIH-PA Author Manuscript
NIH-PA Author Manuscript

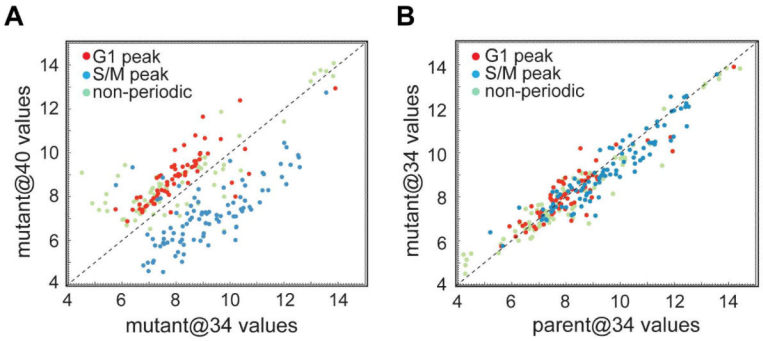

Figure 2. Gene expression analysis confirmed G1 arrest of the mutant 11-104A4 at 40°C

Total RNA from parent and mutant 11-104A4 parasites was obtained following incubation at 34°C (@34) or 40°C (@40), converted to cRNA, and used to hybridize *Toxoplasma* GeneChips (see Experimental Procedures for full details). Published cyclical mRNAs with peak expression in the G1 versus S/M periods (Behnke *et al*., 2010) were evaluated in the parent and mutant hybridization results. In mutant parasites, many transcripts previously shown to peak in G1 were increased by high temperature when compared to growth at 34°C, while the converse was true for S/M peak transcripts **(A)**. S/M transcripts downregulated in the mutant at 40°C included mRNAs encoding invasion genes such as rhoptry and inner-membrane-complex proteins (see Dataset S1 in Supplement for full hybridization results). The temperature-induced skewing of the mRNA pool towards a G1 profile was not observed when comparing the transcripts of parent and mutant parasites replicating at 34°C **(B)**.

NIH-PA Author Manuscript
NIH-PA Author Manuscript
NIH-PA Author Manuscript

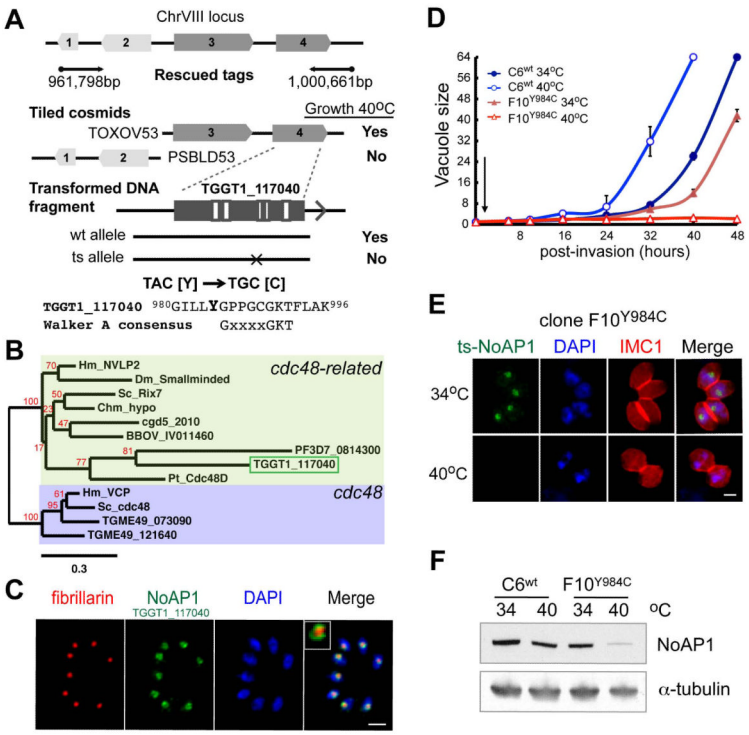

Figure 3. A mutation in a conserved P-loop type NTPase (AAA+ family) is responsible for the conditional growth arrest of mutant 11-104A4

(A) Schematic of the chromosome VIII locus identified by genetic complementation of mutant 11-104A4 parasites (black arrows indicate the position and sequence direction of the marker-rescued tags). The locus identified includes four predicted genes, which was further resolved to either gene #3 (TGGT1_117050) or gene #4 (TGGT1_117040) by successful complementation with cosmid TOXOV53 (Growth 40°C), while cosmid PSBLD53 failed to rescue temperature sensitivity eliminating genes #1-TGGT1_117170 or #2-TGGT1_117060. A third round of complementation resolved the defective gene to TGGT1_117040 (#4) using DNA fragments produced by PCR from genomic DNA (promoter, coding region and 3'UTR sequences). Note only DNA fragments amplified from parental RHΔ*hxgprt* (wt allele) and not from mutant parasites (ts allele) were capable of rescuing mutant 11-104A4 at 40°C. Sequencing of TGGT1_117040 cDNA from mutant 11-104A4 and parental RHΔ*hxgprt* parasites identified a single transversion mutation resulting in a change of tyrosine to cysteine (Y984C; mutated amino acid in bold, see also Fig. S2A). **(B)** Gene TGGT1_117040 (green box) encodes a predicted 1,326 amino acid, P-loop type NTPase that is most similar to nucleolar AAA-NTPases from human (NVL2) and yeast (Rix7) cells, and was therefore designated TgNoAP1 (see supplement Fig. S3 for sequence alignment and Fig. S2A for protein organization). Molecular phylogeny of AAA+ family members including TgNoAP1 compared to canonical cdc48 proteins is shown (Hm=human, Dm=*Drosophila melanogaster*, Chm=*Chlamydomonas reinhardtii*, Pt=*Paramecium tetraurelia*, Sc=*Sacharomyces cervesiae*, cgd=*Cryptosporidium parvum*, BBOV=*Babesia bovis*, Tg=*Toxoplasma gondii*, PF=*Plasmodium falciparum*). Branch support values determined in 500 bootstrap replicates are shown in red. The tree is drawn to scale, with branch lengths determined by the number of substitutions per site. Note that cytoplasmic TgCDC48CY (TGME49_073090) and apicoplast TgCDC48AP (TGME49_121640) were grouped with canonical members of the cdc48 family, while TGGT1_117040 (TgNoAP1) specifically grouped with members of cdc48-related family, including yeast Rix7 and human NVL2

NIH-PA Author Manuscript

NIH-PA Author Manuscript

NIH-PA Author Manuscript

proteins. **(C)** To localize native TgNoAP1 in the parasite, the parental gene allele in RHΔ*ku80* strain was endogenously tagged with a triple copy of the myc epitope by recombination (Huynh & Carruthers, 2009). Clone $C6^{wt}$ expressing $TgNoAP1^{myc}$ was grown for 24 h (37°C) and co-stained with antibodies for the myc epitope (green) and nucleolar core factor fibrillarin (red) as well as for genomic DNA with DAPI (blue). The $TgNoAP1^{myc}$ protein was exclusively nuclear where it localized to the nucleolar compartment in a ring pattern surrounding the nucleolar core occupied by fibrillarin (inset merge image shows the red stain encircled by green). Scale bar = 5μm **(D)** To validate that the mutant ts-TgNoAP1 allele was responsible for conditional growth, the mutation responsible for the Y984C change was introduced into the RHΔ*ku80* strain by gene knock-in, while also epitope tagging the converted ts-TgNoAP1 protein with 3xmyc (clone $F10^{Y984C}$ expressing ts-$TgNoAP1^{myc}$). Rates of parasite division in live cultures were determined for the clone $C6^{wt}$ versus mutant clone $F10^{Y984C}$ following a brief invasion period at 34°C (30 min indicated by arrow) with the number of parasites per vacuole (vacuole size) averaged from 100 randomly selected vacuoles in three independent cultures per strain and temperature condition (34°C=circles, 40°C=triangles). Note that the 48 h time points in the $C6^{wt}$ cultures were not collected due to extensive egress of mature vacuoles. **(E and F)** To understand how the Y984C mutation impacts ts-$TgNoAP1^{myc}$ protein expression, $C6^{wt}$ and $F10^{Y984C}$ parasites were evaluated by IFA and Western analysis at 34°C and 40°C. IFA samples (E) were co-stained with antibodies for αMyc (green, wt- or ts-$TgNoAp1^{myc}$ protein) and αIMC1 (red, whole parasite detection) as well as DAPI (blue, genomic DNA). Scale bar = 2μm. Western blots (F) of $C6^{wt}$ and $F10^{Y984C}$ lysates were probed with αMyc antibodies followed by staining with antibodies against α-tubulin to assess equal loading of parasite extracts.

NIH-PA Author Manuscript
NIH-PA Author Manuscript
NIH-PA Author Manuscript

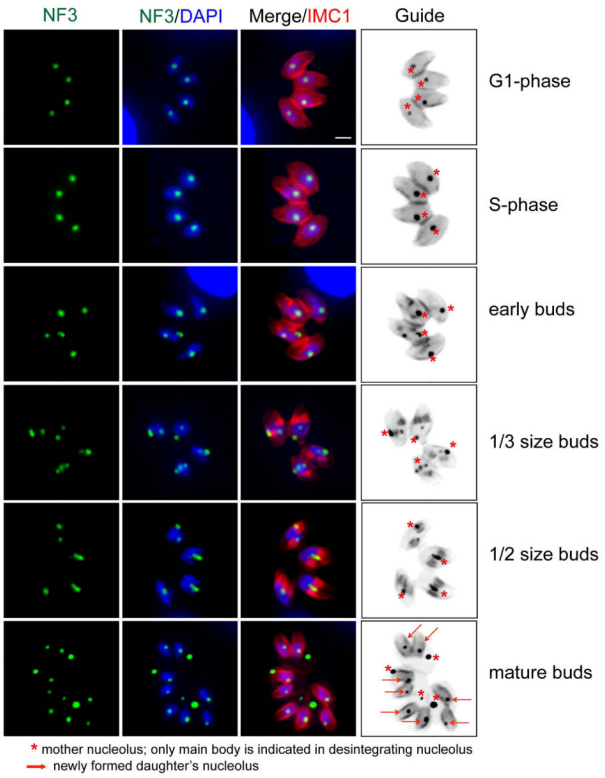

Figure 4. Major morphogenic changes of the nucleolus during tachyzoite replication

Immunofluorescence of factor TgNF3 reveals the tachyzoite nucleolus undergoes dramatic morphogenic changes during parasite division. Nucleolus structure and organization was examined in replicating 11-104A4 parasites (grown at 34°C) first synchronized by limiting invasion (see Experimental Procedures) and then inoculated into cover slips for IFA analysis. At various times, samples were harvested and co-stained with antibodies for TgNF3 and IMC1 as well as stained with DAPI. Representative nucleolar morphology at six cell cycle phases and transitions is shown as identified by established cell cycle criteria based on parasite size and shape (red=IMC1 staining), nuclear morphology (DAPI, single versus double nuclei), and the presence or absence of internal daughters (also red=IMC1). Note immediately following the initiation of budding (early buds), the nucleolus began to fragment with some nucleolar material occasionally lost in the mother cell residual mass. The stars in the marker guide panel (B&W inverse of merged IMC1 and TgNF3 stains), indicates nucleolar material, while the arrows in the bottom guide image indicate the nucleoli of new daughter parasites. Scale bar = 2μm.

NIH-PA Author Manuscript

NIH-PA Author Manuscript

NIH-PA Author Manuscript

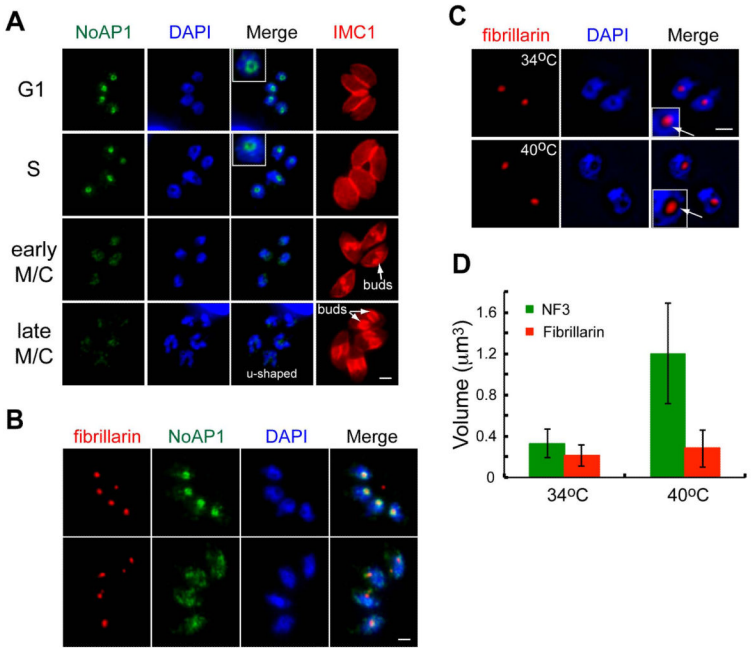

Figure 5. TgNoAP1 is dynamically regulated in the tachyzoite cell cycle

(A) Nucleolar TgNoAP1^{myc} is tightly regulated in the tachyzoite cell cycle (see also Fig. S2C and D) with peak expression in the G1 and S phases followed by a rapid decline in protein levels as parasites progressed through mitosis and cytokinesis. Representative cell cycle stages are shown based on peak expression of TgNoAP1^{myc} in G1 (top image series) or as TgNoAP1^{myc} levels rapidly decreased during the initiation of mitosis and daughter budding (bottom image series). The bottom two-image panels show parasites with internal daughter buds and u-shaped nuclei (bottom DAPI images). Inset images in the G1 and S phase panels show the discrete ring subcompartment of the nucleolus containing TgNoAP1^{myc}. IFA analysis was performed as in Fig. 3E. Scale bar = 2μm. **(B)** Co-staining for TgNoAP1^{myc} (green) and fibrillarin (red) as in Fig. 3C demonstrates that these proteins have distinct fates during parasite division. Note that association of fibrillarin in the nuclear core was relatively stable compared to the normal decline of TgNoAP1^{myc} that occurred at the onset of mitosis in these replicating parasites. Scale bar = 2μm. **(C)** Distinct fates for different nucleolar factors were also observed in ts-TgNoAP1 parasites. Despite the loss of ts-TgNoAP1 at higher temperature, the inner nucleolar core detected by fibrillarin antibody staining was present and similar in mutant parasites (clone F10^{Y984C}) grown at 34°C or growth arrested at 40°C. Scale bar = 2μm. **(D)** Temperature induced increase in nucleolar size in ts-TgNoAP1 parasites at 40°C was reflected in changes in TgNF3, but not fibrillarin staining area. Nucleolus diameter was estimated in the corresponding images of the thirty randomly selected (40°C) or G1/S-phase (34°C) parasites using AxioVision software. These results suggested that the expansion of nucleolar mass caused by the loss of ts-TgNoAP1 in mutant parasites was likely due to specific enlargement of the granular ring.

NIH-PA Author Manuscript

NIH-PA Author Manuscript

NIH-PA Author Manuscript

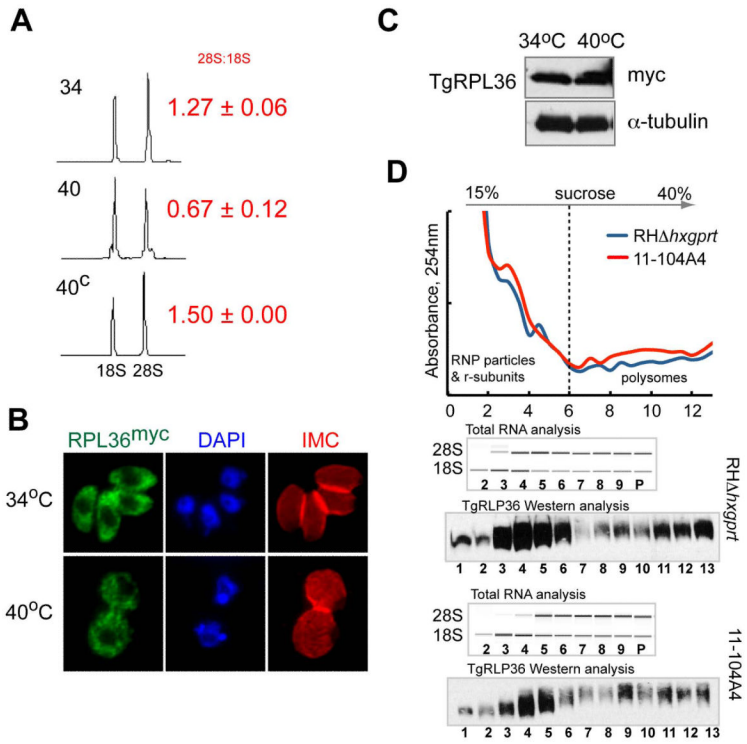

Figure 6. Analysis of ribosome content in the mutant 11-104A4 parasites

To examine whether the loss of ts-TgNoAP1 at high temperature influenced ribosome biogenesis, ribosomal protein and rRNA levels were examined in the original mutant 11-104A4 strain. **(A)** Total RNA was isolated from mutant parasites cultured at permissive and non-permissive temperatures (labeled 34 & 40) and a genetically rescued parasite clone (40^{C}) at the non-permissive temperature only. RNA samples were analyzed on an Agilent Bioanalyzer 2100 (microfluidic analysis) to assess quality and relative levels of the major ribosomal subunit RNAs (18S and ~28S). Chromatograms of the separated rRNA species are shown. The ratio of 28S:18S rRNA measured in three independent experiments is shown to the right of panel. **(B and C)** In order to assess ribosome content and cellular distribution, the gene encoding ribosomal protein TgRPL36 was expressed as a fusion protein with a triple myc epitope (C-terminal) in mutant 11-104A4 parasites. Similar cellular distribution (B) and levels of $TgRPL36^{myc}$ protein in Western blots (C) were detected in mutant parasites incubated for 24 h at 34°C (growing) or 40°C (growth arrested). Probing the Western blot with antibodies to α-tubulin demonstrate equal loading of parasite lysates. Note that the relative strength of the $TgRPL36^{myc}$ fluorescence signal and the cytoplasmic distribution were unaffected by temperature. (**D)** Analysis of ribosomes isolated from parental and mutant 11-104A4 strains expressing $TgRPL36^{myc}$ after 10 h incubation at 40°C. RNP particles and ribosomal subunits were separated from polysomes on the 15-40% sucrose gradient (dashed line). UV-graph of sucrose gradients shows changes in the RNA absorbance at 254nm in the collected fractions. Bioanalyzer microfluidic analysis of the total RNA in fractions 2 to 9 and pooled fractions 10-13 (P) is shown. Western blot analysis shows distribution of the $TgRLP36^{myc}$ in the same gradient fractions. Note that restricted temperature did not change the relative abundance of the RNP particles or translational polysomes in the mutant 11-104A4 defective in TgNoAP1.

NIH-PA Author Manuscript
NIH-PA Author Manuscript
NIH-PA Author Manuscript

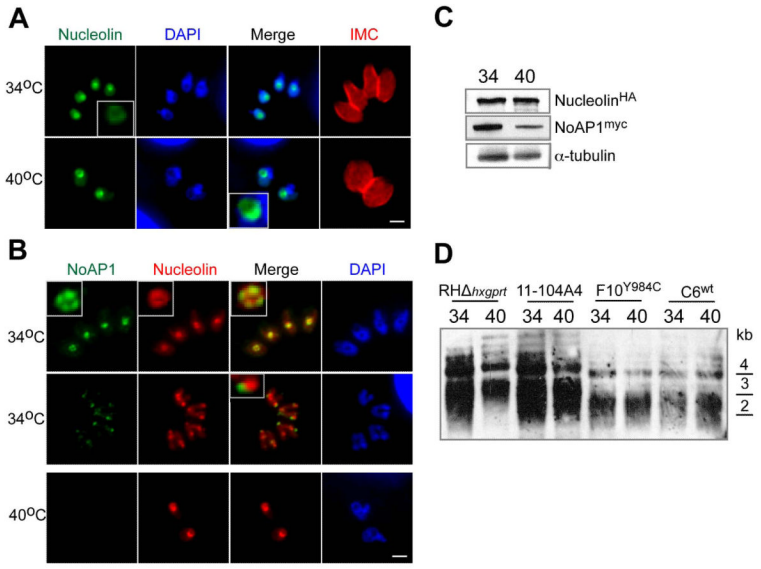

Figure 7. Loss of ts-TgNoAP1 does not effect nucleolin localization or cause temperature-induced changes in telomere lengths

(A and B) *Toxoplasma* nucleolin (TGGT1_031630) was tagged by recombination with a 3xHA epitope in clone F10^{Y984C} resulting in a dual tagged transgenic strain (nucleolin^{HA} and ts-TgNoAP1^{myc}). IFA analysis of this strain at 34°C or 40°C showed that nucleolin^{HA} protein was retained in the parasite nucleolus (A and B image panels). This factor was detected in both the fibrillar core and granular ring based on co-staining of ts-TgNoAP1^{myc} (B panels, see also image insets in 34°C top image series). Interesting, normal fragmentation of the nucleolus (34°C) in mitosis revealed ts-TgNoAP1^{myc} and nucleolin^{HA} were localized to distinct organellar fragments (B panel, see inset in 34°C middle images). **(C)** Western analysis showed that ts-TgNoAP1^{myc} levels decreased at 40°C in the dual-tagged strain, whereas nucleolin^{HA} levels in these same cells was not affected by temperature (see Experimental Procedures for details). Probing of Western blots with antibodies to alpha-tubulin demonstrated equal loading of parasite lysates. **(D)** Examination of telomere length in parental and ts-TgNoAP1 mutant parasites. Genomic DNA was isolated at two temperatures from RHΔ*hxgprt* parent and clone C6^{wt} (wt-TgNoAP1^{myc} expressing) and compared to the original ts-mutant 11-104A4 and the new ts-mutant clone F10^{Y984C} (ts-TgNoAP1^{myc} expressing). Genomic DNA was fragmented by restriction digest and the resulting Southern blot probed for telomere fragments (see Experimental Procedures). DNA standards are indicated to the right of the Southern blot.

NIH-PA Author Manuscript

NIH-PA Author Manuscript

NIH-PA Author Manuscript

Summary of the nucleolar factors identified in TgNoAP1 pull-down

Gene ID TGME49_	Product	Comment
	U3 snoRNP: box C/D	
247470	Nop56	pre-rRNA 2'-O-methylation
205510	Nop58	pre-rRNA 2'-O-methylation
297430	Hypothetical	Fibrillarin; 2'-O-methyltransferase domain
236580	15.5k snoRNP protein	L7A family RNA binding protein
	U3 snoRNP: H/ACA	
313560	RPL7A	L7A family RNA binding protein
	U3 snoRNP assembly	
219590	RuvB family 1 protein	Helicase, R2TP complex
288860	RuvB family 2 protein	Helicase, R2TP complex
251780	HSP70	Chaperone, protein folding
	Other nucleolar proteins	
230710	TgNoAP1	ATPase, AAA family (this study)
311030	UTP10	90S pre-ribosome complex
205580	Nuclear factor NF4	Olguin-Lamas, et al., 2011
260440	Nuclear factor NF3	Olguin-Lamas, et al., 2011
269180	MIF4G domain protein	eIF4A binding protein

Schematic of the snoRNP complexes on the right visualize factors identified in TgNoAP1 pull-down (colored circles). Non-detected subunits indicated with non-colored circles.

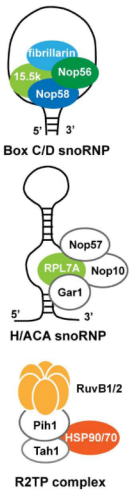

Figure 8. TgNoAP1 precipitated complexes are enriched with nucleolar components involved in the pre-rRNA modification

Nucleolar factors that were found specifically associated with TgNoAP1^{myc} in pulldowns from C6^{wt} clone lysates are indicated. Proteins are grouped into the known nucleolar complexes: the U3 snoRNP assembled either on the box C/D or H/ACA snoRNA secondary structures and the snoRNP assembly factors. Schematic drawing of the complexes is shown in the right panel. Subunits identified in the TgNoAP1 pulldown are shown in color. See Dataset S2 in supplement for complete list of the factors identified in the IP/LC-MS/MS of TgNoAP1^{myc}.

NIH-PA Author Manuscript

NIH-PA Author Manuscript

NIH-PA Author Manuscript

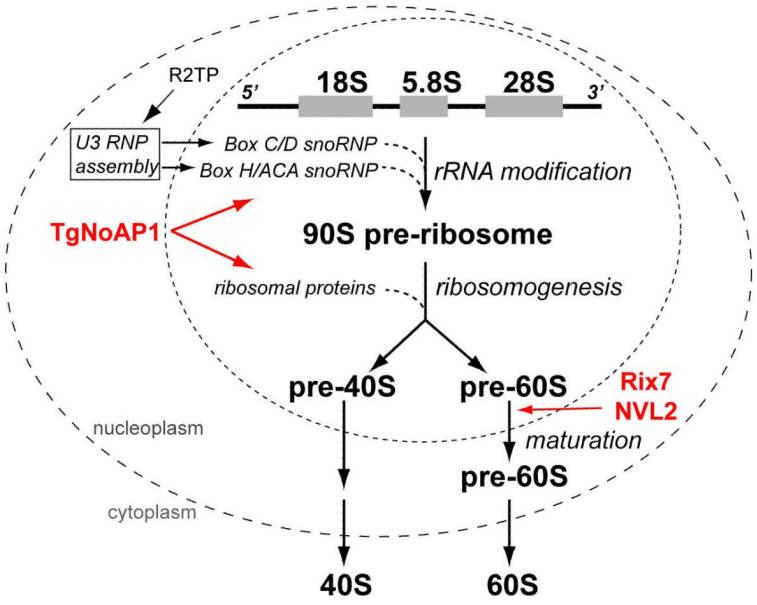

Figure 9. Subcellular localization of the complexes involved in eukaryotic ribosome biogenesis

The multi-stage process of ribosome component synthesis and assembly takes place in three cellular compartments: nucleolus, nucleus and cytoplasm. While rDNA is transcribed in the fibrillar core of the nucleolus, the critical complexes (U3 snoRNP) assisting co-transcriptional modifications of pre-rRNA (box C/D RNA complex catalyzes 2′-O-methylation and H/ACA RNA complex promotes pseudouridine modification) are assembled and translocated from nucleoplasm to nucleolus under control of the R2TP complexes. Ribosomogenesis continues in the nucleolus where maturation of the 90S pre-ribosome particle leads to release of pre-40S and pre-60S ribosomal subunits into the nucleus. The 60S large subunit undergoes additional processing in the nucleoplasm; a step facilitated by the yeast (Rix7) and human (NVL2) orthologs of TgNoAP1. Mature individual small (40S) and large (60S) subunits of the ribosome are released into the cytoplasm. Evidence presented in this study strongly indicates that *Toxoplasma* TgNoAP1 associates with the complexes involved in modification of the pre-rRNA and maturation of the 90S preribosome, which is upstream in ribosome biogenesis from the 60S maturation steps that acquire closely related AAA ATPases, Rix7 and NVL2.